ELECTROMAGNETIC SHIELDING

GENERAL ASPECTS

Electromagnetic shielding represents a way to limit the emission levels of electromagnetic (EM) sources or to protect people or electrical and electronics apparatus and systems against possible effects due to external EM fields. Very often the need for electromagnetic shielding relies not only on functioning motivations but also on the constraints associated with the compliance with standards that fix the limits of emission for various classes of apparatus and systems. Such limitation or protection is generally obtained by means of a structure, often but not necessarily metallic, named the *shield*. The shield performance depends on its geometrical and electrical parameters and on the characteristics of the unperturbed EM field (i.e., the EM field that would exist without any shielding structure, often referred to as *incident*). Various constructive peculiarities affect the performance of the overall shielding system. On a theoretical basis, the shield configurations may be closed or open, depending on whether the source and the (potential) victim are completely separated or not by the shield. The most important factors in determining the performance of a shielding structure are the geometrical configuration and the thickness of the shield and the material, generally characterized by the values of conductivity σ, permeability μ, and permittivity ϵ. Also very important are the so-called discontinuities of the shield such as junctions,

seams, gaps, and apertures, which are always present in practical configurations.

The performance of a shield configuration is often expressed synthetically in terms of *shielding effectiveness* (SE), which is defined by the IEEE dictionary and by military standard MIL-STD 285 as the ratio of electric or magnetic field strength at a point before (E^{i} or H^{i}) and after (E or H) the placement of the shield between a given external source and the considered observation point. In terms of Cartesian coordinates (x_0, y_0, z_0), the following expressions apply:

$$\mathrm{SE}_E = \frac{E^{\mathrm{i}}(x_0, y_0, z_0)}{E(x_0, y_0, z_0)} \tag{1a}$$

$$\mathrm{SE}_H = \frac{H^{\mathrm{i}}(x_0, y_0, z_0)}{H(x_0, y_0, z_0)} \tag{1b}$$

These two figures of merit are usually expressed in decibels, as

$$\mathrm{SE}_{E\,(\mathrm{dB})} = 20\log_{10}\frac{E^{\mathrm{i}}(x_0, y_0, z_0)}{E(x_0, y_0, z_0)} \tag{2a}$$

$$\mathrm{SE}_{H\,(\mathrm{dB})} = 20\log_{10}\frac{H^{\mathrm{i}}(x_0, y_0, z_0)}{H(x_0, y_0, z_0)} \tag{2b}$$

In the case of sinusoidal sources the electric and magnetic field are expressed as root-mean-square (rms) values in the preceding expressions.

The performance of a shield is characterized also by the *shielding factor* (SF), which is defined as the ratio (in decibels) of the total electric or magnetic field on the two surfaces of the shield:

$$\mathrm{SF}_{E\,(\mathrm{dB})} = 20\log_{10}\frac{E^{\mathrm{t}}(x_1, y_1, z_1)}{E^{\mathrm{o}}(x_2, y_2, z_2)} \tag{3a}$$

$$\mathrm{SF}_{H\,(\mathrm{dB})} = 20\log_{10}\frac{H^{\mathrm{t}}(x_1, y_1, z_1)}{H^{\mathrm{o}}(x_2, y_2, z_2)} \tag{3b}$$

where superscripts t and o denote the transmitted and the outgoing fields, respectively, at the first and from the last shield interface. The points at which the fields are evaluated are denoted by the Cartesian coordinates (x_1, y_1, z_1) and (x_2, y_2, z_2), the latter being along the direction of propagation in the shield medium through the former.

Figures 1 and 2 show the configurations leading to the evaluation of SE and SF, respectively. Both these quantities,

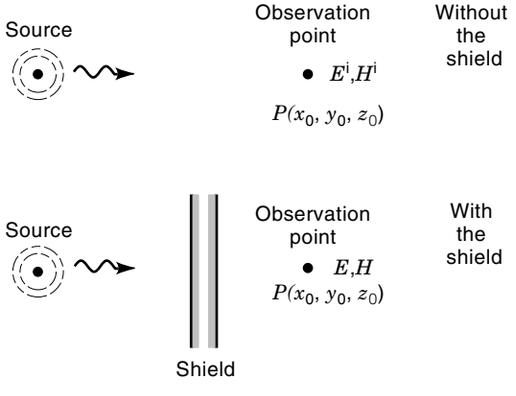

Figure 1. System configurations for the evaluation of the shielding effectiveness SE.

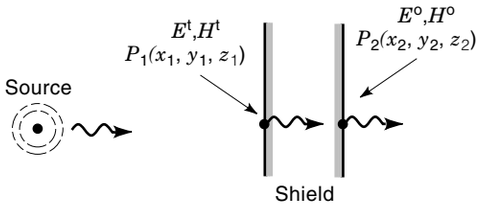

Figure 2. System configuration for the evaluation of the shielding factor SF.

SE and SF, raised some criticism basically because of the problems occurring during their experimental determination. In fact, when measuring the shielding effectiveness SE, the shield may affect the electromagnetic field produced by a real source in the near field. This phenomenon is due to the currents induced on the shield surfaces and may affect measurements by several decibels. On the other hand, the shielding factor SF also cannot be measured easily due to the practical difficulty in placing field sensors on the surface of the shield. The sensors themselves are of finite dimensions and perturb the field distributions. The need for significant but measurable quantities is of paramount importance in the shielding practice, making it possible to verify predictions experimentally and to design shielding structures as well as to promulgate standards.

Shielding theory, including analytical formulations, has been well developed in order to obtain guidance in practical problems and to grasp deeply the key factors upon which the whole electromagnetic problem turns. For the great difficulty of handling real configurations by means of analytical expressions, the analysis of the SE of closed structures is generally performed, either in the frequency or time domain, by using numerical techniques. This may require large computational efforts, depending on the geometrical configuration, the characteristics of the shield material, and the source type, the latter aspect being the starting point of every shielding consideration.

ELECTROSTATICS

An electrostatic field may be easily shielded by means of a conducting enclosure since the charges, which are free to move on the enclosure surface, provide a complete or partial cancellation of the external field when the shield configuration is, respectively, closed or open. The shielding mechanism is represented by the spatial distribution of the charges on the enclosure surface, which tend to cancel the incident electric field, as depicted if Fig. 3. Real enclosures present apertures that may diminish the SE; in order to have an estimation of the SE provided by a conducting shield having a

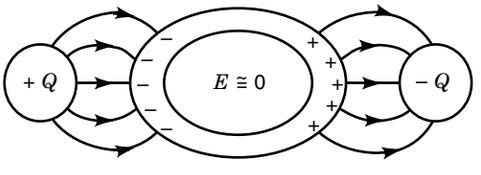

Figure 3. Electrostatic shielding provided by a conductive shell.

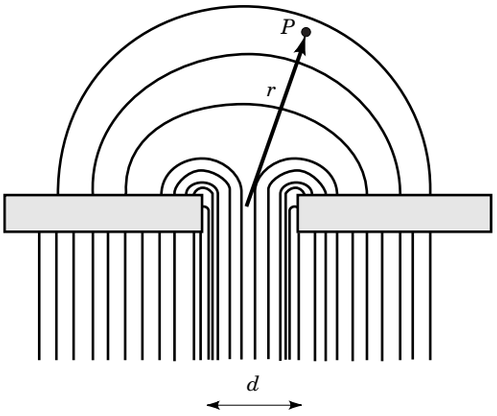

Figure 4. Electrostatic shielding provided by a planar shield with an aperture.

circular hole of diameter d, the following expression may be considered for a uniform incident field valid at a point P located at a distance r from the center of the aperture, far enough compared to d, from the center of the hole, as shown in Fig. 4:

$$\mathrm{SE}_{E\,(\mathrm{dB})} = 20\log_{10}\left(6\pi\frac{r^3}{d^3}\right) \tag{4}$$

The expressions valid for different shapes of the apertures may be found in Refs. 1 and 2.

MAGNETOSTATICS

It is generally much more difficult to shield magnetostatic fields than electrostatic fields because no free magnetic poles exist to counteract the source field. A static magnetic field may be reduced in a prescribed region by means of the following:

1. An active system that is able to produce a magnetic field as opposite to the external one as possible
2. A ferromagnetic shield, which, offering a preferential path, is able to diverge the magnetic field from the interior region as shown in Fig. 5

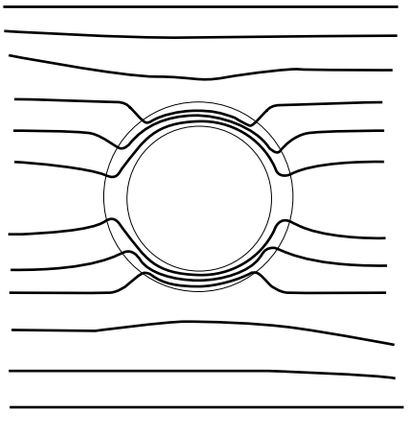

Figure 5. Magnetostatic shielding provided by a ferromagnetic material.

3. A superconducting shield that is able to expel a static magnetic field (3), such an exclusion being practically complete. Even though problems of flux trapping may exist, superconducting shields are highly effective against static and low-frequency magnetic fields.

The second solution is often preferred because of economical and practical reasons, even though the other two ways of shielding a static magnetic field have been implemented.

The magnetic field H^{in} inside a hollow spherical shield by means of a ferromagnetic material may be expressed analytically as a function of the external uniform static field H^{out} (4). In the hypothesis of constant magnetic permeability, the internal field is uniform and the following expression can be used:

$$\frac{H^{\mathrm{out}}}{H^{\mathrm{in}}} = 1 + \frac{2}{9\mu_{\mathrm{r}}}(\mu_{\mathrm{r}} - 1)^2\left(\frac{d}{R}\right)^3 \tag{5}$$

where μ_{r}, d, and R are the relative magnetic permeability, the thickness, and the external radius of the shield, respectively. Different shield shapes will result in a distortion of the internal field and no analytical expressions are available; however, an approximate equivalent radius can be estimated. For instance, the value giving the best approximation for the magnetic field in the center of a cubic shield is that corresponding to a sphere of the same volume (5).

An analytical solution is also available for the ideal configuration of an infinite cylindrical shield in a uniform field transverse to the shield axis (4):

$$\frac{H^{\mathrm{out}}}{H^{\mathrm{in}}} = \frac{1}{4\mu_{\mathrm{r}}}\left[(\mu_{\mathrm{r}} + 1)^2 - (\mu_{\mathrm{r}} - 1)^2\left(\frac{r}{R}\right)^2\right] \tag{6}$$

where r and R represent, respectively, the inner and outer radius of the cylindrical shield. For real cylinders of finite length, Eq. (6) is a valid approximation only if the length of the shield is much greater than its diameter.

ELECTROMAGNETICS

When the electric and the magnetic fields are coupled via Maxwell equations, another mechanism that can increase the shield is present, because time-varying magnetic fields give rise to induced currents the effects of which tend to oppose to their cause. Of course the shielding mechanisms described for static fields are still present, with the importance of the various contributions being dependent upon the frequency, the thickness, the conductivity, and the magnetic permeability of the shield as well as on its transverse dimensions. The solution of the shielding problem can be obtained by considering various approaches, which may be cast into two main classes: analytical and numerical. Among the analytical methods used to solve shielding problems, the most relevant and successful are the direct solution of the Maxwell equations governing the system and the so-called transmission-line approach, proposed by Schelkunoff (6).

Direct Solution of Maxwell Equations

The direct solution of the equations governing the shielding problem is available only in a few simple configurations. How-

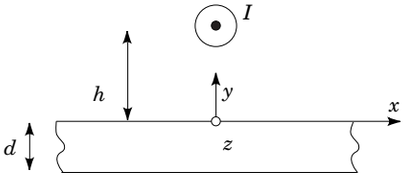

Figure 6. Shielding of the electromagnetic field due to an infinite wire current by means of a planar shield.

ever, some relevant cases with reasonable assumptions may be studied in this way. Moreover, such exact solutions may serve as a reference for other methods and thus represent a fundamental tool in shielding analyses. Among the system configurations for which an analytical solution of the Maxwell equations has been found, there are those depicted in Figs. 6 and 7. Other relevant configurations are analyzed in Refs. 7 and 8. Also, the ideal configuration of a planar shield of infinite extension and illuminated by a plane wave admits an exact solution, as will be described in detail subsequently.

Infinite Line Source—Infinite Conducting Plane. Without the shield, the electric and the magnetic fields in free space due to an infinite wire current are given by the following expressions in cylindrical coordinates (9):

$$E_z = -I\frac{\omega\mu}{4}H_0^{(2)}(\beta\rho) \tag{7a}$$

$$H_\varphi = -I\frac{j\beta}{4}H_1^{(2)}(\beta\rho) \tag{7b}$$

where ω is the radian frequency of the sinusoidal current in the wire, $H_0^{(2)}$ and $H_1^{(2)}$ are the Hankel functions of the second kind of order 0 and 1, respectively, and $\beta = \omega/c$ is the phase constant, with c the field propagation velocity in free space. When the shield is applied, the problem is solved in terms of magnetic vector potential in the three regions above, inside and below the shield, as shown in Fig. 6. The magnetic vector potential only has the z component. In the hypothesis that displacement currents in the shield may be neglected by imposing the continuity of the normal component of the magnetic flux density and the continuity of the tangential component of the magnetic field, the magnetic vector potential beyond a shield of thickness d is obtained (10) as

$$A_z(x,y) = \frac{2\mu_0 I}{\pi}\int_0^\infty \frac{\lambda(\alpha)e^{\alpha(y+d)}e^{-\alpha h}\cos(\alpha x)}{[\lambda(\alpha)+\mu_r\alpha]e^{\lambda(\alpha)d} - [\lambda(\alpha)-\mu_r\alpha]e^{-\lambda(\alpha)d}}\,d\alpha \tag{8}$$

where $\lambda(\alpha) = \sqrt{\alpha^2 + j\omega\mu\sigma}$ and I is the rms value of the sinusoidal current flowing in the source conductor. Then, the magnetic and electric fields beyond the shield are readily obtained, and both SE and SF easily computed considering that

$$\boldsymbol{H}(x,y) = \frac{1}{\mu_0}\nabla\times\boldsymbol{A}(x,y) \tag{9a}$$

$$\boldsymbol{E}(x,y) = -j\omega\boldsymbol{A}(x,y) \tag{9b}$$

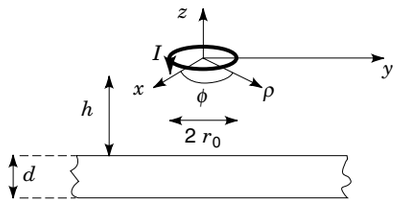

Figure 7. Shielding of the electromagnetic field due to the current flowing in a circular loop by means of a planar shield.

Current Loop Source in a Plane Parallel to an Infinite Planar Shield. The analysis procedure to solve the configuration shown in Fig. 7 has been presented in Ref. 11. The electric and magnetic fields due to the source in free space are given in cylindrical coordinates as

$$E_\varphi = -\frac{j\omega\mu_0 r_0 I}{2}\int_0^\infty \frac{\alpha}{\tau_0}J_1(\alpha r_0)J_1(\alpha\rho)e^{-\tau_0 z}d\alpha \tag{10a}$$

$$H_\rho = \frac{r_0 I}{2}\int_0^\infty \alpha J_1(\alpha r_0)J_1(\alpha\rho)e^{-\tau_0 z}d\alpha \tag{10b}$$

$$H_z = \frac{r_0 I}{2}\int_0^\infty \frac{\alpha^2}{\tau_0}J_1(\alpha r_0)J_0(\alpha\rho)e^{-\tau_0 z}d\alpha \tag{10c}$$

where $\tau_0 = \sqrt{\alpha^2 - \omega^2\mu_0\epsilon_0}$, J_0 and J_1 are the Bessel functions of the first kind of order 0 and 1, respectively, r_0 is the radius of the loop source, and I is the rms value of the sinusoidal current flowing in the loop. These expressions are valid when the current in the loop may be considered uniform, that is, it does not vary with the angle coordinate φ. When the shield is applied, the analytical solution may be found in Ref. 11, and the following expressions hold for the electric and magnetic fields beyond the shield:

$$E_\varphi = -2j\omega\mu_0 r_0 I\int_0^\infty \frac{C\alpha\tau}{\tau_0^2}J_1(\alpha r_0)J_1(\alpha\rho)e^{-\tau_0 z-(\tau-\tau_0)d}d\alpha \tag{11a}$$

$$H_\rho = 2r_0 I\int_0^\infty \frac{C\alpha\tau}{\tau_0}J_1(\alpha r_0)J_1(\alpha\rho)e^{-\tau_0 z-(\tau-\tau_0)d}d\alpha \tag{11b}$$

$$H_z = 2r_0 I\int_0^\infty \frac{C\alpha^2\tau}{\tau_0^2}J_1(\alpha r_0)J_0(\alpha\rho)e^{-\tau_0 z-(\tau-\tau_0)d}d\alpha \tag{11c}$$

where

$$\tau = \sqrt{\alpha^2 - j\omega\mu\sigma} \tag{11d}$$

$$C(\alpha) = \left[\left(\frac{\tau}{\tau_0}+\mu_r\right)^2 - \left(\frac{\tau}{\tau_0}-\mu_r\right)^2 e^{-2\tau d}\right]^{-1} \tag{11e}$$

Other geometrical shapes of relevant practical interest are the spherical and the infinitely long cylindrical shield in a magnetic field that is uniform before the insertion of the shields. Under the assumptions that the shield thickness is much smaller than the shield radius and that the shield radius is much smaller than the wavelength of the electromagnetic field, the following two expressions hold for spherical and cylindrical shields, respectively (4),

$$\frac{H^{\text{out}}}{H^{\text{in}}} = \cosh(\gamma d) + \frac{1}{3}\left(A + \frac{2}{A}\right)\sinh(\gamma d) \tag{12a}$$

$$\frac{H^{\text{out}}}{H^{\text{in}}} = \cosh(\gamma d) + \frac{1}{2}\left(A + \frac{1}{A}\right)\sinh(\gamma d) \tag{12b}$$

where $\gamma = \sqrt{j\omega\mu_0\mu_r\sigma}$, $A = \gamma r_m/\mu_r$, and d and r_m are, respectively, the thickness and the mean radius of the shield.

Transmission Line Approach

This method was initially introduced with reference to a plane wave impinging with a normal angle of incidence on an infinite planar shield and successively extended to cope with other source and shield configurations. The method is based on the analogy existing between the equations governing voltage and current in a transmission line and those describing the electric and the magnetic field propagation inside a planar shield subjected to a plane wave, as shown in Fig. 8. Considering a sinusoidal field source, the problem may be solved in the frequency domain, provided that the shield material is linear. For a normal angle of incidence of a plane wave having only the y component of the electric field and the z component of the magnetic field, Maxwell curl equations governing the field propagation through the shield become

$$\frac{dE_y}{dx} = -j\omega\mu H_z \tag{13a}$$

$$\frac{dH_z}{dx} = -(\sigma + j\omega\epsilon)E_y \tag{13b}$$

It is readily recognized that the equation system (13) describes the electric and magnetic field propagation as well as the voltage and current propagation in a transmission line, when reading voltage and current instead of E_y and H_z, respectively, and substituting $j\omega\mu$ and $\sigma + j\omega\epsilon$ with the per-unit length impedance and admittance of the line, respectively. The electric and magnetic fields inside the shield material, $E_y(x)$ and $H_z(x)$ at the generic distance x from the first interface between air and shield are expressed as functions of the corresponding quantities at $x = 0$:

$$E_y(x) = E_y(0)\cosh(\gamma x) - \eta H_z(0)\sinh(\gamma x) \tag{14a}$$

$$H_z(x) = -\frac{1}{\eta}E_y(0)\sinh(\gamma x) + H_z(0)\cosh(\gamma x) \tag{14b}$$

where η is the intrinsic impedance of the shield given by

$$\eta = \left(\frac{j\omega\mu}{\sigma + j\omega\epsilon}\right)^{1/2} \tag{15}$$

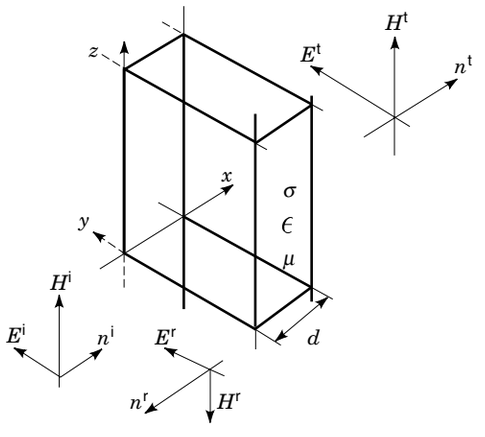

Figure 8. Shielding of a plane-wave electromagnetic field by means of a planar shield.

and γ is the propagation constant of the electromagnetic field inside the shield:

$$\gamma = [j\omega\mu(\sigma + j\omega\epsilon)]^{1/2} \tag{16}$$

The system is solved by applying adequate boundary conditions. Usually, such boundary conditions are applied considering the continuity of the tangential components of the electric and magnetic field incident on the shield surfaces, which are also the only components propagating through the shield by virtue of the Poynting theorem. In the considered configuration, they read

$$E_y^i + E_y^r = E_y^t \quad \text{at } x = 0 \tag{17a}$$

$$H_z^i - H_z^r = H_z^t \quad \text{at } x = 0 \tag{17b}$$

$$E_y^t = E_y^o \quad \text{at } x = d \tag{17c}$$

$$H_z^t = H_z^o \quad \text{at } x = d \tag{17d}$$

where the superscripts i, r, t, and o denote, respectively, the incident, reflected, transmitted, and outgoing fields. The incident field is due to the source alone, the reflected field is due to the contribution of the induced currents on the shield surface, the transmitted field is the field propagating through the shield medium, and the outgoing field is passed behind the shield.

Uniform Plane-Wave Field Source. A uniform plane wave is, by definition, a wave in which the electric and magnetic fields are perpendicular to each other, their direction of propagation does not vary in time, and their amplitude is constant in space and in time. It is of course an idealization because the EM field produced by real sources must decay in space, but if the observation point is very far from the real source, that is, if its distance is much greater than the wavelength of the electromagnetic field, the uniform plane-wave assumption is quite realistic. In a plane wave both incident and reflected electric and magnetic fields stay in a fixed ratio, which is defined as the wave impedance Z_w of the EM field:

$$Z_w = \frac{E_y^i}{H_z^i} = \frac{E_y^r}{H_z^r} = \frac{E_y^o}{H_z^o} = \sqrt{\frac{\mu_0}{\epsilon_0}} = 120\pi\ \Omega \cong 377\ \Omega \tag{18}$$

Equations (17b) and (17d), prescribing the continuity of the tangential components of the magnetic field, are multiplied by Z_w, and the results are added to Eqs. (17a) and (17c), respectively, in order to find the relationships between the incident and the transmitted fields at the two shield interfaces:

$$2E_y^i = E_y^t + Z_w H_z^t \quad \text{at } x = 0 \tag{19a}$$

$$0 = E_y^t - Z_w H_z^t \quad \text{at } x = \mathrm{d} \tag{19b}$$

In this way the reflected fields, which are generally unknown and not always easy to evaluate, do not appear in the boundary conditions. It is evident that Eqs. (19a) and (19b) are formally identical to those valid for a real voltage source and a simple load impedance, allowing the use of the analogy with a transmission line also as concerns the boundary conditions. In the case of a uniform plane wave presenting an oblique angle of incident on a shield surface, the problem may be solved by considering that an arbitrarily oriented wave may

be split into various waves, each formed by the orthogonal electric and magnetic field components propagating along different directions (12). The use of the superposition principle, provided the shield material is linear, allows for an easy realization of all the possible physical situations. It is worth noting that, with reference to the coordinate system shown in Fig. 8, the two waves constituted by (E_y, H_z) and (E_z, $-H_y$) propagate toward the shield and have to be accounted for in shielding analyses, the other waves being responsible for a sliding in directions parallel to the shield. Thus, two wave impedances are considered to extend the previous formulation to the oblique incidence case:

$$Z_{w1} = \frac{E_y}{H_z} \tag{20a}$$

$$Z_{w2} = -\frac{E_z}{H_y} \tag{20b}$$

These two wave impedances are used to impose the boundary conditions (19a) and (19b) and allow the evaluation of the total electric and magnetic field components transmitted beyond the shield.

Near-Field Sources. In order to analyze the performance of shields against near-field sources, it is useful to introduce the elementary EM field sources known as the electric and the magnetic dipole. Although these sources are ideal, that is, they do not exist in the real world, nevertheless the EM field they produce is easy to determine and very similar to that of some common real sources. The EM field produced by these sources depends strongly on the distance r from the observation point. In fact, the amplitude of the electric field due to an electric dipole is expressed, in spherical coordinates, as the sum of three terms depending on $1/r$, $1/r^2$, and $1/r^3$, respectively, whereas the magnetic field is function of $1/r$ and $1/r^2$ only:

$$E_r^i(r,\omega) = \sqrt{\frac{\mu_0}{\epsilon_0}}\frac{I(\omega)L}{4\pi}2\cos(\theta)\left(\frac{1}{r^2}+\frac{1}{j\beta r^3}\right)e^{-j\beta r} \tag{21a}$$

$$E_\theta^i(r,\omega) = \sqrt{\frac{\mu_0}{\epsilon_0}}\frac{I(\omega)L}{4\pi}\sin(\theta)\left(\frac{j\beta}{r}+\frac{1}{r^2}+\frac{1}{j\beta r^3}\right)e^{-j\beta r} \tag{21b}$$

$$E_\varphi^i(r,\omega) = 0 \tag{21c}$$

$$H_r^i(r,\omega) = 0 \tag{21d}$$

$$H_\theta^i(r,\omega) = 0 \tag{21e}$$

$$H_\varphi^i(r,\omega) = \frac{I(\omega)L}{4\pi}\sin(\theta)\left(\frac{j\beta}{r}+\frac{1}{r^2}\right)e^{-j\beta r} \tag{21f}$$

where $I(\omega)$ is the current flowing in the elementary source of length L. Therefore, at points far from an electric dipole (far-field region), that means at a distance r from the EM source much greater than the wavelength λ, the term proportional to $1/r$ prevails in both the expressions of the electric and magnetic field, so that their ratio, representing the wave impedance Z_w at a distance r, assumes the same value of a uniform plane wave, that is, 377 Ω. In contrast, in the near-field region, where $r/\lambda \ll 1$, the terms proportional to $1/r^3$ and $1/r^2$ are the dominant ones in the electric and magnetic field expressions, respectively. Consequently, the wave impedance Z_w is a function of the position and of the frequency; its value is generally greater than 377 Ω and the electric dipole is termed the high-impedance source. Magnetic dipoles present characteristics that are dual with respect to electric dipoles. The amplitude of the radiated magnetic field is expressed as the sum of three terms depending on $1/r$, $1/r^2$, and $1/r^3$, respectively, whereas the electric field is function of $1/r$ and $1/r^2$ only:

$$E_r^i(r,\omega) = 0 \tag{22a}$$

$$E_\theta^i(r,\omega) = 0 \tag{22b}$$

$$E_\varphi^i(r,\omega) = -\frac{j\omega\mu_0 I(\omega)A}{4\pi}\sin(\theta)\left(\frac{j\beta}{r}+\frac{1}{r^2}\right)e^{-j\beta r} \tag{22c}$$

$$H_r^i(r,\omega) = \frac{j\beta I(\omega)A}{4\pi}2\cos(\theta)\left(\frac{1}{r^2}+\frac{1}{j\beta r^3}\right)e^{-j\beta r} \tag{22d}$$

$$H_\theta^i(r,\omega) = \frac{j\beta I(\omega)A}{4\pi}\sin(\theta)\left(\frac{j\beta}{r}+\frac{1}{r^2}+\frac{1}{j\beta r^3}\right)e^{-j\beta r} \tag{22e}$$

$$H_\varphi^i(r,\omega) = 0 \tag{22f}$$

where $I(\omega)$ is the current flowing in the loop with surface A. In the far-field region, the EM field is characterized by the free-space wave impedance. Conversely, in the near-field region, the terms proportional to $1/r^3$ and $1/r^2$ are the dominant ones in the magnetic and electric fields, respectively, and the wave impedance Z_w is lower than 377 Ω. For this reason, the magnetic dipole represents a low impedance source.

In Fig. 9, the trends of the wave impedances of an electric and a magnetic dipole are reported as functions of the distance, normalized by λ, of the observation point from the source.

These considerations are of great importance in extending the transmission line approach to solve near-field source problems. It should be noted that generally the electric and the magnetic fields are not perpendicular to each other, and the various components directed toward the shield, according to the Poynting theorem, may be accounted for separately, as described for the oblique incidence of uniform plane waves. As with the considerations carried out for the oblique incidence of a plane wave on a planar shield, the wave impedances association with the various directions may be defined and utilized to determine the field incident onto a prefixed

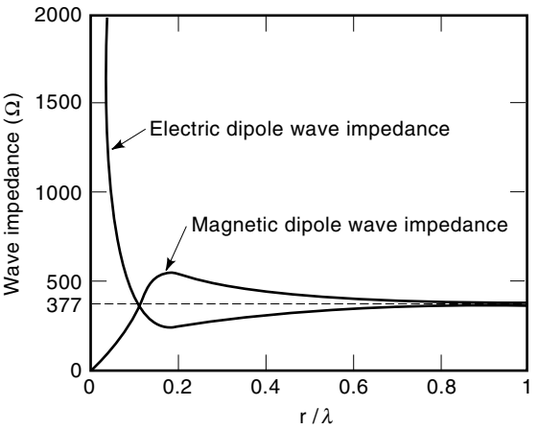

Figure 9. Trend of the wave impedances associated with electric and magnetic dipoles, as a function of the normalized distance from the sinusoidal elemental source.

shield surface. In fact, the boundary conditions may be imposed following the procedure described for the plane-wave source, provided that the electric and the magnetic fields are considered space and frequency dependent (13).

Shielding Effectiveness Evaluation. In the case of uniform plane waves, since the electromagnetic field amplitudes remain constant in space, SE_E and SE_H are numerically coincident. Moreover, the shielding effectiveness differs from the shielding factor by a constant quantity. SE may be stated in the following very compact form (14):

$$SE = A + R + B \tag{23}$$

where the absorption loss A, reflection loss R, and the multiple reflections coefficient B are, respectively, given in decibel by

$$A_{dB} = 20 \log_{10} |e^{\gamma d}| \tag{24a}$$

$$R_{dB} = 20 \log_{10} |(Z_w + \eta)^2 (4 Z_w \eta)^{-1}| \tag{24b}$$

$$B_{dB} = 20 \log_{10} \left| 1 - \frac{(Z_w - \eta)^2}{(Z_w + \eta)^2} e^{-2\gamma d} \right| \tag{24c}$$

The absorption loss coefficient A_{dB} is a function of the shield characteristics only, and the reflection loss coefficient R_{dB} depends upon the mismatch between the wave impedance and the intrinsic impedance of the shield. The multiple reflections coefficient B_{dB} depends on both physical characteristics of the shield material and on the incident field. The coefficient A_{dB} can be put in the following simple form:

$$A_{dB} = 131.44 \sqrt{f \mu_r \sigma_r}\, d \tag{25}$$

Different expressions hold for coefficient R for plane-wave sources, high-impedance sources, and low-impedance sources, respectively:

$$R_{dB} = 168.1 - 20 \log_{10} \sqrt{\frac{f \mu_r}{\sigma_r}} \tag{26a}$$

$$R_{dB} = 321.7 - 10 \log_{10} \left(\frac{\sigma_r}{f^3 \mu_r r^2} \right) \tag{26b}$$

$$R_{dB} = 20 \log_{10} \left(5.35 \sqrt{\frac{\sigma_r f}{\mu_r}} r + 0.0117 \sqrt{\frac{\mu_r}{\sigma_r f}} \frac{1}{r} + 0.5 \right) \tag{26c}$$

where μ_r and σ_r denote, respectively, the relative magnetic permeability and the relative conductivity (with respect to the conductivity of copper $\sigma_{Cu} = 5.8 \times 10^7$ S/m) of the material. Figure 10 shows the absorption loss coefficient A_{dB} as function

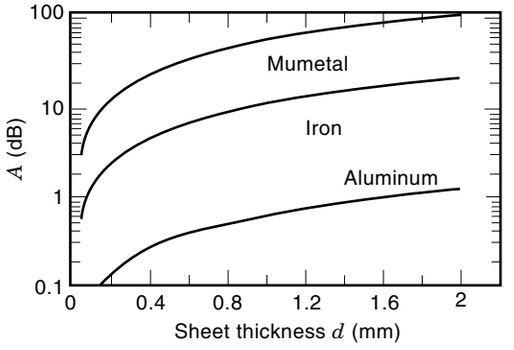

Figure 10. Absorption loss coefficient A_{dB}, as a function of the shield thickness, for various materials at 50 Hz.

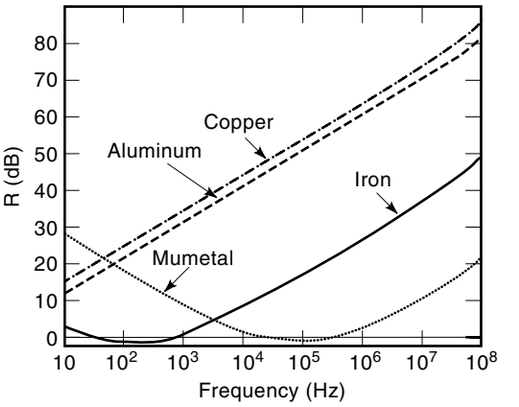

Figure 11. Frequency spectrum of the reflection loss coefficient R_{dB} for various materials against a low-impedance source (permeability assumed constant with frequency).

of the sheet thickness for different materials often used in shielding electromagnetic fields. Figures 11 and 12 show the frequency dependence of coefficient R_{dB} of various materials against low- or high-impedance fields, respectively. Figure 13 shows the frequency dependence of coefficient B_{dB} in case of a low-impedance source. It is worth noting that, in case of low-impedance source, the reflection loss coefficient exhibits values increasing with the frequency, for copper and aluminum, while for ferromagnetic materials it initially decreases and then increases. In the case of a high-impedance source, the trend of the reflection loss coefficient is always decreasing for all the materials. The values of R_{dB} are much lower in the low-impedance source case, confirming the difficulty to shield magnetic fields in time-harmonic low-frequency situations. It should be noted also that the previous expressions are rigorously valid for a plane-wave source impinging normally onto a shield that is conductive, infinite, and planar. When extending the transmission line approach to waves with an oblique angle of incidence, another hypothesis is necessary: the electromagnetic field propagation inside the shield must occur normal to the shield surface; this assumption is gener-

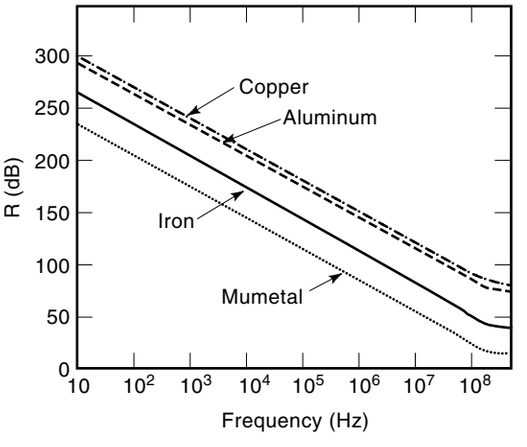

Figure 12. Frequency spectrum of the reflection loss coefficient R_{dB} for various materials against a high-impedance source (permeability assumed constant with frequency).

ally satisfied in consideration of the high values of conductivity, as stated by Snell's law of refraction (9)

$$\gamma_0 \sin(\theta_i) = \gamma_s \sin(\theta_s) \tag{27}$$

where γ_0 and γ_s are, respectively, the propagation constant in air and in the shield medium and θ_i and θ_s the directions of propagation of the electromagnetic field in the two media, respectively. Details regarding the validity of the transmission line approach may be found in Ref. 32.

Other Factors Affecting Shielding Performance. The methods previously described are based upon the assumption that no discontinuities (e.g., apertures, holes, junctions, seams, and so forth) are present in the shield; nevertheless such a hypothesis is quite unrealistic because intentional apertures for various purposes and unintentional defects always exist and may degrade considerably the real shield's performance. No general theory is available to account for such discontinuities; however, some studies have been conducted to quantify the EM field transmitted through intentional apertures of some regular shapes. In fact, when the aperture is electrically small and the shield is perfectly conducting, its contribution to the EM field beyond the shield may be represented as that due to a combination of appropriate elementar electric and magnetic dipoles, located in the centre of the aperture with the shield removed (1,2). Periodically perforated shields have been also studied to some extent (15). Measured data and an intuitive but approximate formulation have been also presented to quantify the effect of various types of discontinuity in EM penetrable shields (14,16), extending the transmission line approach. Figure 14 shows the two paths for the electromagnetic field to penetrate inside a shield with a discontinuity. Since the two paths are present simultaneously, the total electromagnetic field beyond the barrier may be evaluated as the sum of the field transmitted through the solid sheet plus the field penetrating through the discontinuity, the former being evaluated as per the transmission line approach, the latter as suggested in Refs. 1 and 2 if the discontinuity is an aperture or as described in Refs. 14 and 16 if the discontinuity is of another type. Also finiteness of planar shields may be accounted for as described in Ref. 8.

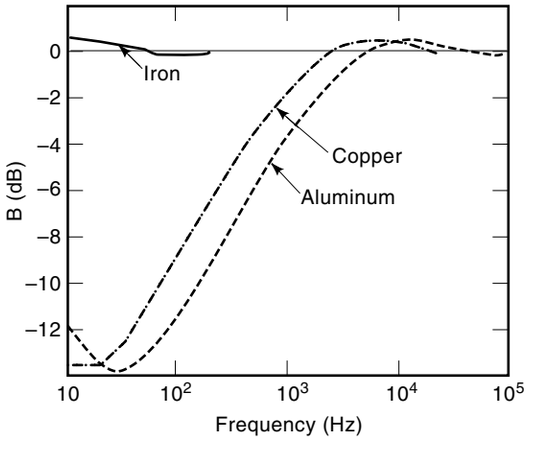

Figure 13. Frequency spectrum of the multiple reflections coefficient B_{dB} for various materials against a low-impedance source (permeability assumed constant with frequency).

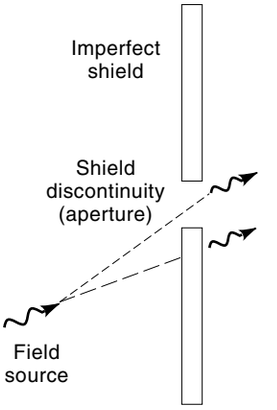

Figure 14. Transmission paths for the electromagnetic field propagating through a planar shield with a discontinuity.

SHIELDING PERFORMANCE MEASUREMENT AND STANDARDS

The most common documents describing the test procedures recommended to assess the shielding characteristics of enclosures are the following:

- Military Standard (MIL-STD) 285: Method of attenuation measurements for enclosures and electromagnetic shielding, for electronic test purposes
- National Security Agency (NSA) Specification 65-6: General specifications for RF-shielded enclosures for communications equipment
- National Security Agency (NSA) Specification 73-2: General specifications for foil RF-shielded enclosures for communications equipment
- IEEE 299: Standard method of measuring the effectiveness of electromagnetic shielded enclosures

All these documents describe antenna geometries and configurations as well as delineate some measurements practices, classifying the source as magnetic, electric, or plane-wave type. It is important to put in evidence that the data obtained considering any of the previously described setups cannot be applied to source configurations different from those used in the experiments. Thus, they have only reference value (17).

Figures 15 and 16 show, respectively, the configurations prescribed by MIL-STD 285 and NSA 65-6 for the measurement of the SE against a magnetic field source. The different loop antenna setup should be noted: the two loops are coplanar in the first configuration and coaxial in the second. Figures 17 and 18 show the configurations requested in the measurements of the SE against an electric field source and a plane wave source, respectively.

As concerns shielding materials, the most used standards are as follows: IEC 60093 (1980-01), methods of test for volume resistivity and surface resistivity of solid electrical insulating materials; and ASTM D 4935-89 (1994), standard test

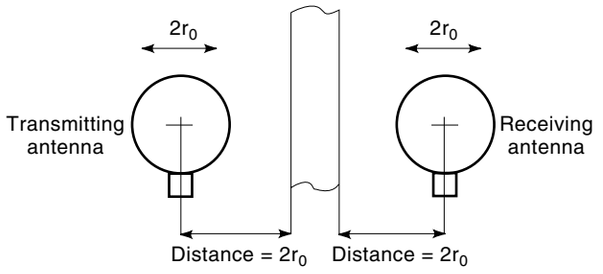

Figure 15. Experimental configuration for the measurement of the magnetic field shielding effectiveness, according to MIL-STD 285.

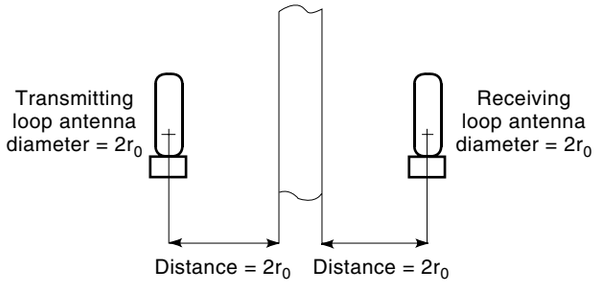

Figure 16. Experimental configuration for the evaluation of the magnetic field shielding effectiveness, according to NSA 65-6.

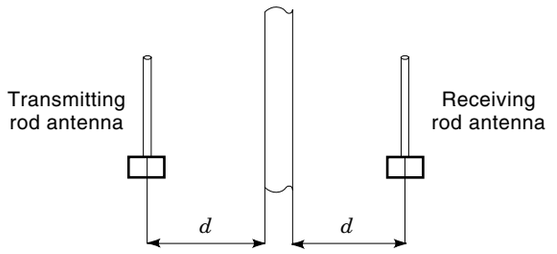

Figure 17. Experimental configuration for the evaluation of the electric field shielding effectiveness, according to NSA 65-6.

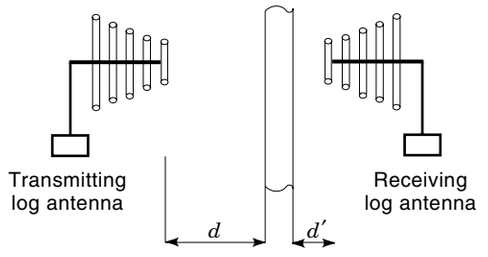

Figure 18. Experimental configuration for the evaluation of the plane-wave field shielding effectiveness, according to NSA 65-6.

method for measuring the electromagnetic shielding effectiveness of planar materials.

NUMERICAL METHODS FOR SHIELDING ANALYSIS

The intrinsic limitations of analytical formulations has lead to a wide literature concerning studies on the application of various numerical methods to shielding problems, an exhaustive report being practically impossible. However, examples of the application of the method of moments to shielding configurations may be found in Ref. 18 and 19, while the finite difference time domain method has been applied in Refs. 20–22, the boundary element method in Ref. 23, the transmission line method in Ref. 24, and the finite element method in Ref. 25. Concerning the last numerical technique, it is worth mentioning the approach proposed in Refs. 26 and 27, which is valid when the EM field distribution inside a conducting penetrable shield enclosure illuminated by an external field is sought. The method avoids the numerical costs associated with the fine discretization of the metallic regions and the imposition of adequate boundary conditions where the mesh is truncated. The philosophy underlying the method is similar to that of Thevenin theorem in circuit theory: since the main interest lies in the evaluation of the EM field in the shielded region, the shield itself and the external region, where the source is located, are replaced by adequate equivalent boundary conditions. For instance, considering a TE-polarized plane-wave electromagnetic field impinging with different angles of incidence and different phases on the various edges of the enclosure, the new boundary conditions are given in terms of an equivalent electric field source characterized by an equivalent wave impedance:

$$E_{\mathrm{eq}k}^{\mathrm{TE}}(d_k) = \frac{2\eta_k E_{zk}^{\mathrm{TE,i}}}{\eta_k \cosh(\gamma_k d_k) + \eta_{0k}^{\mathrm{TE}} \sinh(\gamma_k d_k)} \tag{28a}$$

$$\eta_{\mathrm{eq}k}^{\mathrm{TE}}(d_k) = \eta_k \frac{\eta_{0k}^{\mathrm{TE}} + \eta_k \tanh(\gamma_k d_k)}{\eta_k + \eta_{0k}^{\mathrm{TE}} \tanh(\gamma_k d_k)} \tag{28b}$$

where

$$\eta_{0k}^{\mathrm{TE}} = \eta_0 \sec(\theta_k) \tag{28c}$$

$$\gamma_k = [j\omega\mu_k(\sigma_k + j\omega\epsilon_k)]^{1/2} \tag{28d}$$

$$\eta_k = \left(\frac{j\omega\mu_k}{\sigma_k + j\omega\epsilon_k}\right)^{1/2} \tag{28e}$$

With reference to Fig. 19, $E_{zk}^{\mathrm{TE,i}}$ is the electric field impinging on the kth edge of the enclosure, d_k is the thickness of the same edge, and θ_k is the angle of incidence of the external

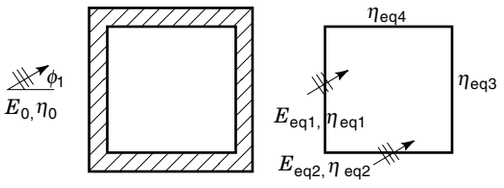

Figure 19. Enclosure illuminated by a plane wave and region of interest with equivalent boundary conditions.

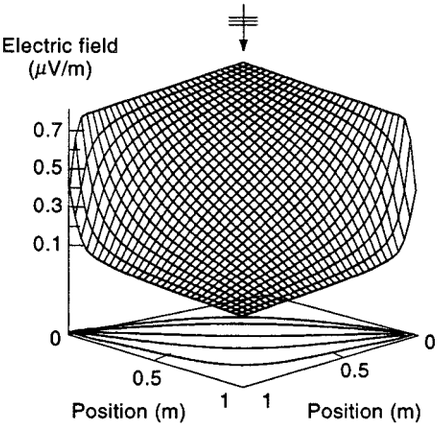

Figure 20. Electric field inside a square enclosure illuminated by a plane wave having $\theta_i = \pi/4$ and $E^i = 1$ V/m.

field. These boundary conditions are applied on the internal sides of the enclosure removing the enclosure itself and the exterior region. The method has been applied also to the time-domain analysis of multiple shields. Figure 20 shows the map of the electric field inside the square cavity shown in Fig. 19, considering four sheets of length 1 m, thickness $d = 25$ μm, and conductivity $\sigma = 10^4$ S/m, against a TE-polarized plane-wave field of amplitude 1 V/m with an angle of incidence $\theta_1 = \pi/4$.

CURRENT RESEARCH TOPICS

Various aspects of electromagnetic shielding are currently under investigation. One of the most challenging research topics is the analysis and the design of real shielding structures (28,29). In particular, low-frequency magnetic fields are shielded with difficulty and often by means of nonlinear and expensive ferromagnetic materials, requiring computer-aided design of shielding structures.

Another important field of research is the development of new synthetic materials providing good performance; in particular, to mention just two examples, large efforts are made to find composite materials that have not only excellent mechanical properties but also good shielding characteristics. Optically transparent materials having good shielding performance are sought also.

As already mentioned, the correct way to extend and use data referred to standard configurations in different source configurations is an aspect of paramount importance, having tight links with standard development and preparation and greatly affecting meaning and usability of published data. Of course, ways to perform measurements for the characterization of both materials (30,31) and shielding structures are always under investigation.

Finally, since all the previously mentioned research topics need the formulation of work hypotheses and their successive experimental verification, numerical modeling and analysis methods are continuously compelled to deal with more complex materials and configurations and thus their improvement represents a fundamental research topic in electromagnetic shielding.

BIBLIOGRAPHY

1. F. De Meulenaere and J. van Bladel, Polarizability of some small apertures, *IEEE Trans. Antennas Propag.,* **25**: 198–205, 1977.
2. K. S. H. Lee (ed.), *EMP Interaction: Principles, Techniques and Reference Data,* New York: Hemisphere, 1989.
3. J. M. Blatt, *Theory of Superconductivity,* New York: Academic Press, 1964.
4. L. V. King, Electromagnetic shielding at radio frequencies, *Philos. Mag.,* Ser. 7, **15**: 201–223, 1933.
5. A. K. Thomas, Magnetic shielded enclosure design in the DC and VLF region, *IEEE Trans. Electromagn. Compat.,* **10**: 142–152, 1968.
6. S. A. Schelkunoff, *Electromagnetic Waves,* New York: Van Nostrand, 1943.
7. J. J. Bowman, T. B. A. Senior, and P. L. E. Uslenghi, *Electromagnetic Scattering by Simple Shapes,* New York: Hemisphere, 1987.
8. R. G. Olsen and P. Moreno, Some observations about shielding extremely low-frequency magnetic fields by finite width shields, *IEEE Trans. Electromagn. Compat.,* **38**: 460–468, 1996.
9. C. A. Balanis, *Advanced Engineering Electromagnetics,* New York: Wiley, 1989.
10. J. A. Tegopoulos and E. E. Kriezis, *Eddy Currents in Linear Conducting Media,* Amsterdam: Elsevier, 1985.
11. J. R. Moser, Low-frequency low-impedance electromagnetic shielding, *IEEE Trans. Electromagn. Compat.,* **30**, 202–210, 1988.
12. R. A. Adler, L. J. Chu, and R. M. Fano, *Electromagnetic Energy Transmission and Radiation,* New York: Wiley, 1960.
13. S. Celozzi and M. D'Amore, Magnetic field attenuation of nonlinear shields, *IEEE Trans. Electromagn. Compat.,* **38**: 318–326, 1996.
14. R. B. Schulz, V. C. Plantz, and D. R. Brush, Shielding theory and practice, *IEEE Trans. Electromagn. Compat.,* **30**: 187–201, 1988.
15. K. F. Casey, Electromagnetic shielding behavior of wire-mesh screens, *IEEE Trans. Electromagn. Compat.,* **30**: 298–306, 1988.
16. R. B. Schulz, V. C. Plantz, and D. R. Brush, Low-frequency shielding resonance, *IEEE Trans. Electromagn. Compat.,* **10**: 7–15, 1968.
17. J. E. Bridges, Proposed recommended practices for the measurement of shielding effectiveness of high-performance shielding enclosures, *IEEE Trans. Electromagn. Compat.,* **10**: 82–94, 1968.
18. H. Singer, H. D. Bruns, and G. Burger, State of the art in the method of moments, Proceedings of the *IEEE 1996 Int. Symp. Electromagn. Compat.,* Santa Clara, 1996, pp. 122–127.
19. G. Burger, H. D. Bruns, and H. Singer, Simulation of thin layers in the method of moments, *Proc. 11th Int. Zurich Symp.,* Zurich, Switzerland, 1995, pp. 339–344.
20. R. J. Luebbers, et al., FDTD calculation of transient pulse propagation through a nonlinear magnetic sheet, *IEEE Trans. Electromagn. Compat.* **33**: pp. 90–94, 1993.
21. M. Li, et al., Numerical and experimental corroboration of an FDTD thin-slot model for slots near corners of shielding enclosures, *IEEE Trans. Electromagn. Compat.,* **39**: pp. 225–232, 1997.
22. A. Taflove, *Computational Electrodynamics: The Finite-Difference Time-Domain Method,* Boston: Artech House, 1995.
23. J. Shen and A. Kost, Hybrid FE-BE Method for EMC problems in cable systems, *IEEE Trans. Magn.* **32**: 1493–1496, 1996.
24. A. Mallik, D. P. Johns, and A. J. Wlodarczyk, TLM modelling of wires and slots, *Proc. 10th Int. Zurich Symp.,* Zurich, Switzerland, 1993, pp. 515–520.
25. L. B. Gravelle and G. I. Costache, Finite element method applied to shielding performance of enclosure, *Proc. IEEE 1988 Int. Symp. Electromagn. Compat.,* Seattle, 1988, pp. 69–72.

26. S. Celozzi and M. D'Amore, A new approach to predict shielding properties of layered nonlinear sheets, *Proc. IEEE 1994 Int. Symp. Electromagn. Compat.,* Chicago, 1994, pp. 42–47.
27. S. Celozzi and M. S. Sarto, Equivalent source method for the evaluation of the electromagnetic field penetration inside enclosures, *IEEE Trans. Magn.,* **32**: 1497–1500, 1996.
28. J. A. Catrysse, Comparative study of different combinations of metallized flexible shielding materials under mechanical stress, *Proc. 12th Int. Zurich Symp.,* Zurich, Switzerland, 1997, pp. 235–238.
29. J. A. Catrysse, Comparative study of different combinations of metallized non-woven shielding materials and an insulating substrate, for use as shielding envelopes and small shielding boxes, *Proc. Int. Symp. Electromagn. Compat.* EMC '96 ROMA, Rome, Italy, 1996, pp. 569–573.
30. P. F. Wilson and M. T. Ma, Shielding effectiveness measurements with a dual TEM cell, *IEEE Trans. Electromagn. Compat.,* **27**: 137–142, 1985.
31. J. A. Catrysse and C. P. J. H. Borgmans, Measuring methods and measuring setups for the characterisation of shielding materials under different conditions, *Proc. Int. Symp. Electromagn. Compat. EMC '96 Roma,* Rome, Italy, 1996, pp. 562–568.
32. A. C. D. Whitehouse, Screening: new wave impedance for the transmission line analogy, *IEE Proc.,* **116**: 1159–1164, 1969.

Reading List

First Special Issue on Electromagnetic Shielding, *IEEE Trans. Electromagn. Compat.,* **10**: No. 1, 1968.

L. H. Hemming, *Architectural Shielding,* New York: IEEE Press, 1992.

K. C. Lin, et al., Integral law descriptions of quasistatic field shielding by thin conducting plates, *IEEE Trans. Power Deliv.,* **12**: 1642–1650, 1997.

Second Special Issue on Electromagnetic Shielding, *IEEE Trans. Electromagn. Compat.,* **30**: No. 3, 1988.

F. M. Tesche, M. V. Ianoz, and T. Karlsson, *EMC Analysis Methods and Computational Models,* New York: Wiley, 1997.

J. L. Violette, D. R. J. White, and M. F. Violette, *Electromagnetic Compatibility Handbook,* New York: Van Nostrand, Reinhold Co., 1987.

SALVATORE CELOZZI
University of Rome "La Sapienza"
MARCELLO D'AMORE
University of Rome "La Sapienza"